Available online at www.sciencedirect.com
SCIENCE DIRECT®
Surface Science 550 (2004) 199–212
SURFACE SCIENCE
www.elsevier.com/locate/susc

A quantum chemical study of ZrO_2 atomic layer deposition growth reactions on the SiO_2 surface

Joseph H. Han [a], Guilian Gao [b], Yuniarto Widjaja [a], Eric Garfunkel [c], Charles B. Musgrave [d,*]

[a] *Department of Chemical Engineering, Stanford University, Stanford, CA 94305-5025, USA*
[b] *Materials Science Department, Ford Research Laboratory, Ford Motor Company, Dearborn, MI 48121, USA*
[c] *Department of Chemistry, Rutgers University, Piscataway, NJ 08854, USA*
[d] *Departments of Chemical Engineering and Materials Science and Engineering, Stanford University, 381 North-South Mall, Stanford, CA 94305-5025, USA*

Received 25 February 2003; accepted for publication 10 December 2003

Abstract

Zirconium oxide (ZrO_2) is one of the leading candidates to replace silicon oxide (SiO_2) as the gate dielectric for future generation metal-oxide-semiconductor (MOS) based nanoelectronic devices. Experimental studies have shown that a 1–3 monolayer SiO_2 film between the high permittivity metal oxide and the substrate silicon is needed to minimize electrical degradation. This study uses density functional theory (DFT) to investigate the initial growth reactions of ZrO_2 on hydroxylated SiO_2 by atomic layer deposition (ALD). The reactants investigated in this study are zirconium tetrachloride ($ZrCl_4$) and water (H_2O). Exchange reaction mechanisms for the two reaction half-cycles were investigated. For the first half-reaction, reaction of gaseous $ZrCl_4$ with the hydroxylated SiO_2 surface was studied. Upon adsorption, $ZrCl_4$ forms a stable intermediate complex with the surface SiO_2–OH^* site, followed by formation of SiO_2–O–Zr–Cl^* surface sites and HCl. For the second half-reaction, reaction of H_2O on SiO_2–O–Zr–Cl^* surface sites was investigated. The reaction pathway is analogous to that of the first half-reaction; water first forms a stable intermediate complex followed by evolution of HCl through combination of a Cl atom from the surface site and an H atom from H_2O. The results reveal that the stable intermediate complexes formed in both half-reactions can lead to a slow film growth rate unless process parameters are adjusted to lower the stability of the complex. The energetics of the two half-reactions are similar to those of ZrO_2 ALD on ZrO_2 and as well as the energetics of ZrO_2 ALD on hydroxylated silicon. The energetics of the growth reactions with two surface hydroxyl sites are also described.

Keywords: Density functional calculations; Growth; Surface chemical reaction; Zirconium; Silicon; Halides; Silicon oxides

1. Introduction

SiO_2 has been the gate dielectric of choice for MOS devices for decades because it is easy to grow, is thermally stable, and has a low defect density interface with excellent device electrical

* Corresponding author. Tel.: +1-650-725-9176; fax: 1-650-725-7294.
E-mail address: chasm@stanford.edu (C.B. Musgrave).

0039-6028/$ - see front matter © 2003 Elsevier B.V. All rights reserved.
doi:10.1016/j.susc.2003.12.030

properties; however, the scaling of MOS devices will soon require sub-nanometer SiO_2 effective oxide thickness (EOT) gate dielectrics. SiO_2 dielectrics will no longer be viable as the gate insulator because current leakage via direct tunneling through the dielectric will become too large. Oxynitrides (SiO_xN_y) offer some improvements over pure SiO_2 and are now used commercially, but they too are rapidly reaching fundamental limits. Therefore, there is an urgent need to develop alternative high permittivity (high-κ) gate dielectrics to replace SiO_2 [1]. Using a high-κ material in place of SiO_2 allows one to structure a dielectric film whose EOT is, for example, less than 1 nm yielding a high capacitance, yet has a physical thickness where tunneling is insignificant. Candidate materials that have high permittivity and are thought to be thermally stable on Si include Al_2O_3, ZrO_2, HfO_2, Y_2O_3, La_2O_3, and a few other materials. ZrO_2 is attractive as it has a bulk permittivity of approximately 25 and has been well studied for other applications. In addition to its high dielectric constant, ZrO_2 films have been shown to be stable with respect to reaction with substrate (or overlayer) silicon to temperatures as high as 900 °C [2]. This is an important property because some processing steps after gate dielectric deposition can reach temperatures as high as 1000 °C.

Atomic layer deposition (ALD) is a deposition method for growing thin films of various semiconducting, insulating, and metallic materials with very high conformality and precise thickness control [3]. The deposition technique is based on alternating exposure of a surface to two or more gas phase precursors. The precursors are chosen such that, at an appropriate temperature, they react with the other precursor adsorbed on the surface but not with themselves. Atomic level control is achieved because the reaction of each precursor with the surface in each reaction half-cycle is self-terminating, hence yielding at most one monolayer of added species for each half-cycle. The inherent precise control of the deposition rate makes ALD an ideal choice for deposition of gate dielectrics. ALD has been actively investigated for deposition of ZrO_2 and HfO_2 [2,4–10] for which $ZrCl_4$ and $HfCl_4$, respectively, and H_2O are often used as precursors.

Experimental results over the past three years have shown that the starting surface is critical in initiating growth and assuring uniformity for both ALD and CVD-grown high-κ films. The final properties of the film are strongly regulated by the composition of the film in the interfacial region between the high-κ oxide and the silicon substrate. The best films to date have had at least a few monolayers of SiO_2 present between the high-κ and the substrate silicon. Although this lowers the total capacitance of the stack, interface electrical properties that affect channel mobility seem much better with SiO_2 at the interface. On the other hand, ALD and CVD growth are often accompanied by an initiation period. The problem is that the two halves of the ALD cycle are often much more reactive with each other than with the substrate. What is found for many starting surfaces is non-uniform nucleation, followed by rapid growth of the initial nuclei leading to clusters, rather than the desired case of a full flat homogeneous monolayer with each reaction half-cycle. It is thus critical to understand the reactivity of each species (actually each precursor) on all possible surface species (including defects) that may present themselves to the incident precursor molecule. One must understand the full chemistry, not just the atomic composition: a hydrogen species present at Si–H on the surface is many orders of magnitude less reactive than one present as Si–OH, as we now know.

In one study (typical of many) ZrO_2 deposited on a thin native SiO_2 film was shown to have approximately five orders of magnitude improvement in the leakage current at an equivalent oxide thickness (EOT) of 1.4–1.5 nm [5] compared to a film grown on the oxide-free H-terminated surface. Even when SiO_2 is removed by HF cleaning before initiating the ALD process, a thin SiO_2 film is still often observed between the Si surface and the high-κ dielectric, possibly from oxidation of the Si surface due to the presence of water during the early stages of the ALD process.

In previously reported work, we have studied mechanisms of initiation of ZrO_2 deposition on the clean Si surface using the B3LYP DFT method [11] and ALD of ZrO_2 on ZrO_2, which represents growth of ZrO_2 beyond the first monolayer using

the B3LYP DFT method [12]. Minor energetic differences are found between reactions of $ZrCl_4$ and H_2O on hydroxylated Si and ZrO_2 surfaces. The activation barrier for the $ZrCl_4$ reaction on the hydroxylated Si surface is 1.4 kcal/mol lower than on ZrO_2, and the activation barrier of the H_2O reaction is 1.1 kcal/mol higher on Si than on ZrO_2. Since SiO_2 is present below the deposited ZrO_2 film even after removal of the native oxide by HF cleaning, the deposition of the first monolayer of ZrO_2 may take place on SiO_2. Since the predicted ZrO_2 ALD kinetics of the growing film [12] are not significantly different from the predicted initial ALD rates on hydroxylated Si [11], ALD of ZrO_2 on SiO_2 will most likely not differ significantly from ZrO_2 deposition on either hydroxylated Si or hydroxylated ZrO_2. However, since energetic differences would affect the optimum process conditions for the initial deposition versus ALD of the growing film, verifying the actual reaction kinetics of ZrO_2 on SiO_2 can guide development of ALD processes to produce high quality ZrO_2 films. Consequently, exploring the growth mechanism and associated energetics of the major ZrO_2 ALD growth reactions on SiO_2 is the subject of this investigation. We note that the general behavior of ZrO_2 and HfO_2 deposition are remarkably similar; the subtle differences that do exist will be discussed elsewhere.

2. Calculational details

The reactions between the gaseous precursors $ZrCl_4$ and H_2O with the hydroxylated SiO_2 surface are predicted to proceed via an exchange mechanism [3,9] and can be separated into the two half-reactions:

$$SiO_2\text{–}OH^* + ZrCl_4 \rightarrow SiO_2\text{–}O\text{–}ZrCl_3^* + HCl \quad (1)$$

$$SiO_2\text{–}O\text{–}Zr(OH)_{3-x}\text{–}Cl_x^* + H_2O \rightarrow SiO_2\text{–}O\text{–}Zr(OH)_{4-x}\text{–}Cl_{x-1}^* + HCl \quad (2)$$

where * denotes the active surface species and x has values of 1–3. It should be noted that after the second half-reaction, it is possible for hydroxyl groups on neighboring zirconium atoms to undergo a dehydration reaction thereby decreasing the hydroxyl density on the ZrO_2 surface; this effect will be described in a future publication [13].

To study the surface reactions, we performed DFT quantum chemical simulations of reactions on cluster models of the surface. The B3LYP gradient-corrected hybrid method was used for all calculations. The effectiveness and accuracy of this method for studying transition metals have been investigated by Eriksson et al. [14]. Zirconium, silicon, and chlorine were described using the Los Alamos LANL2DZ basis set (effective core potential, or ECP, and a double-ζ valence shell) [15–17]. We found through preliminary studies that the addition of polarization functions on light atoms can significantly improve the description of bond energies. As such, hydrogen and oxygen were described using the Dunning D95(d,p) basis set [18]. The geometry is optimized by finding stationary points followed by frequency calculations needed to verify the nature of the stationary points on the potential energy surface (PES), to calculate the zero-point energy corrections, and to obtain the thermochemical properties at finite temperatures. The clusters were not constrained during the final transition state (TS) searches. All the calculations were performed using Gaussian 98 [19].

For the first stage of this study, we used the $Si(OH)_3$–OH and $Si(OH)_3OZr(OH)_{3-x}$–Cl_x clusters, where x has values of 1–3, to represent the SiO_2–OH^* and SiO_2–O–Zr–Cl^* surface sites, respectively. The relatively small sizes of these clusters greatly speed up the calculations so that mechanisms can be investigated practically. However, the small size may adversely affect the quality of the results. To determine the reliability of the results predicted by the smaller clusters and evaluate the cluster size effect, we also used the larger clusters $SiH_3OSi(OH)_2$–OH, $(SiH_3O)_3Si$–OH, $SiH_3OSi(OH)_2OZr(OH)_{3-x}$–$Cl_x$ and $(SiH_3O)_3SiO$-$Zr(OH)_{3-x}$–Cl_x. These larger clusters allowed us to investigate the effect of nearby atoms on the energetics of reactions at active SiO_2–OH^* and SiO_2–Zr–Cl^* sites, mimicking the electronic and mechanical effects of the surrounding material of a model hydroxylated SiO_2 surface. All of the clusters used are shown in Fig. 1. Results are

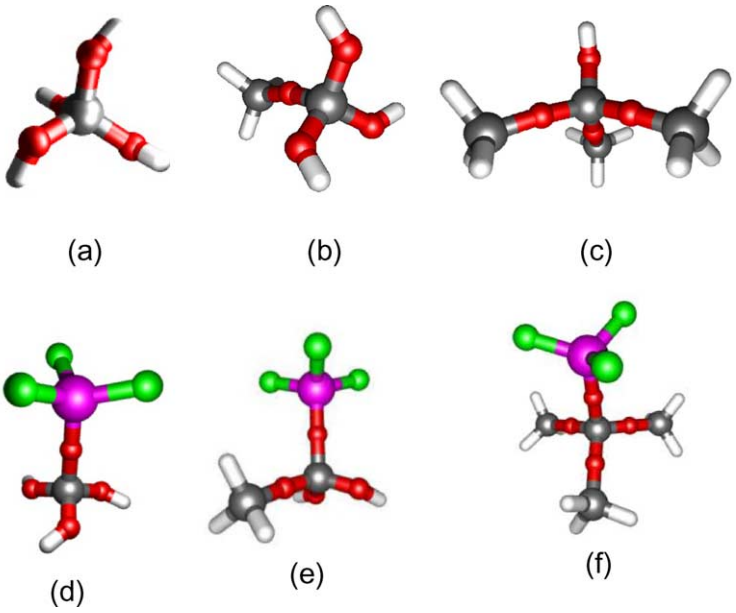

Fig. 1. The (a) $Si(OH)_3$–OH, (b) $SiH_3OSi(OH)_2$–OH, (c) $(SiH_3O)_3Si$–OH, (d) $Si(OH)_3OZrCl_3$, (e) $SiH_3OSi(OH)_2OZrCl_3$ and (f) $(SiH_3O)_3SiOZrCl_3$ clusters used in this study.

compared to the energetics of analogous reactions of ZrO_2 deposition on hydroxylated Si and ZrO_2.

To investigate the reaction of $ZrCl_4$ with multiple surface hydroxyl groups, a $Si(OH)_2$–OH^*–O–$Si(OH)_2$–OH^* cluster is used to represent two surface hydroxyl groups separated by a siloxane bridge. Based on results from the previous calculations in this work, the termination of the Si atoms with –OH groups is sufficient to capture the chemisty of the extended surface. Finally, calculations are also performed on clusters similar to those used by Jeloaica et al. [10] in order to compare their results of ZrO_2 deposition with those of this work.

3. Results and discussion

3.1. Reaction of $ZrCl_4$ with SiO_2–OH^* surface sites

The PES of the reaction of $Si(OH)_3$–OH + $ZrCl_4$, representing reactions of gaseous $ZrCl_4$ on SiO_2–OH^* surface sites, is shown in Fig. 2. Note that this PES is schematic in the sense that only stationary points are calculated and the curve drawn connecting these states is only indicative of the reaction path. $ZrCl_4$ first adsorbs molecularly onto the hydroxylated SiO_2 surface and forms a stable complex with the SiO_2–OH^* surface group. Widjaja and Musgrave [11,12] have shown that a similar complex is formed between $ZrCl_4$ and hydroxyl groups on Si and ZrO_2 through the interaction between the oxygen lone-pair electrons and an empty d-orbital of the Zr atom. This results in a stable intermediate with a formation energy of −16.9 kcal/mol. The complex formation energies are −21.4 kcal/mol on Si and −28.1 kcal/mol on ZrO_2. Following the formation of this intermediate complex, one Cl atom of the adsorbed $ZrCl_4$ combines with the H atom of the surface OH group, forming HCl. The activation barrier for the HCl formation is 16.4 kcal/mol with respect to the energy of the SiO_2–OH–$ZrCl_4$(a) adsorbed complex, and the formation of the HCl is endothermic by 11.9 kcal/mol relative to the adsorbed complex. The activation barrier for HCl formation is 20.0 kcal/mol on Si and 21.3 kcal/mol on ZrO_2 with respect to the adsorbed complex, while HCl formation is endothermic by 13.9 kcal/mol on Si and 16.7 kcal/mol on ZrO_2, both with respect to the

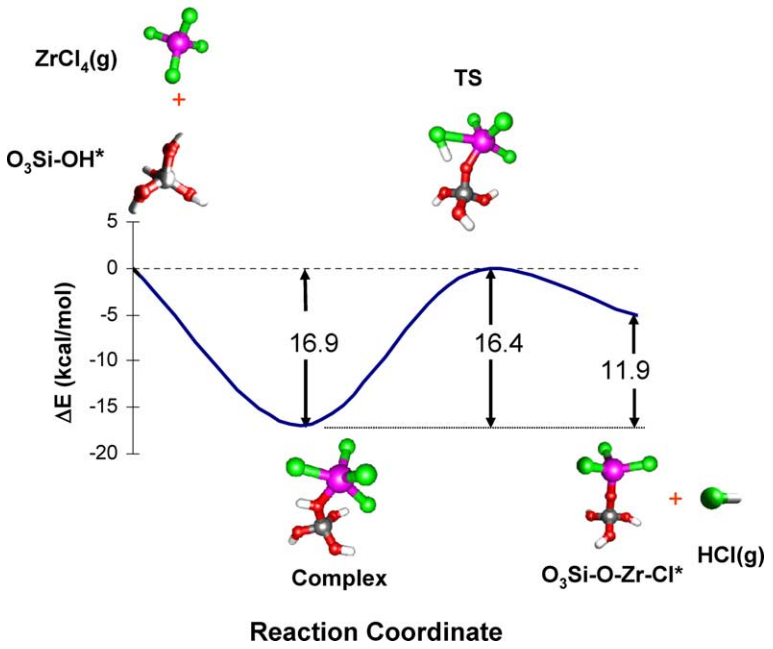

Fig. 2. Reaction path and predicted energetics for the reaction of gaseous $ZrCl_4$ on SiO_2–OH^* sites. The purple, gray, red, green, and white atoms denote the zirconium, silicon, oxygen, chlorine and hydrogen atoms, respectively. (For interpretation of the references in colour in this figure legend, the reader is referred to the web version of this article.)

adsorbed complex. The HCl may go through a weakly bound physisorbed state, and then desorb into the gas phase as it does on Si and ZrO_2. The physisorbed state has not been found for reactions on SiO_2–OH^* sites. The end result of the $ZrCl_4$ reaction with the SiO_2–OH^* site, represented by $Si(OH)_3$–O–$ZrCl_3$, is the replacement of the OH group of the SiO_2–OH^* surface site with three Zr–Cl^* bonds.

3.2. Reaction of H_2O with SiO_2–O–$Zr(OH)_{3-x}Cl_x^*$ surface sites

The atomistic mechanism of the reaction of H_2O+$Si(OH)_3$–O–$ZrCl_3$, representing the reaction of H_2O on SiO_2–O–Zr–Cl^* sites and removal of the first of the three Cl atoms bonded to Zr, is illustrated in Fig. 3. The reaction also proceeds through a trapping-mediated mechanism. Water first forms a stable complex with the Zr atom of SiO_2–O–Zr–Cl^* through donation of the lone-pair electrons of the oxygen atom of water into an empty d-orbital of the Zr atom. The adsorbed state is again stable; the H_2O adsorption reaction is exothermic by 18.0 kcal/mol. The physisorbed HCl(a) state is then formed through the reaction of one H atom from the incoming H_2O and a Cl atom from the SiO_2–O–$ZrCl_3$ surface site. The energy of the transition state leading to the formation of HCl(a) is 20.3 kcal/mol relative to the adsorbed state and the reaction is endothermic by 17.3 kcal/mol relative to the complex. Physisorbed HCl(a) then desorbs with a desorption energy of 1.2 kcal/mol uphill relative to the physisorbed state. Reaction of H_2O on Si and ZrO_2 follows a similar pathway with an HCl desorption energy of 3.1 kcal/mol on Si and 4.5 kcal/mol on ZrO_2.

Removal of the second and third Cl atoms from the active SiO_2–O–Zr–$(OH)_{3-x}Cl_x^*$ sites proceeds through an analogous trapping-mediated mechanism. Formation of an absorbed H_2O complex is followed by reaction of one Cl atom with one H atom from water to form physisorbed HCl. The final results of the reactions are replacements of Cl

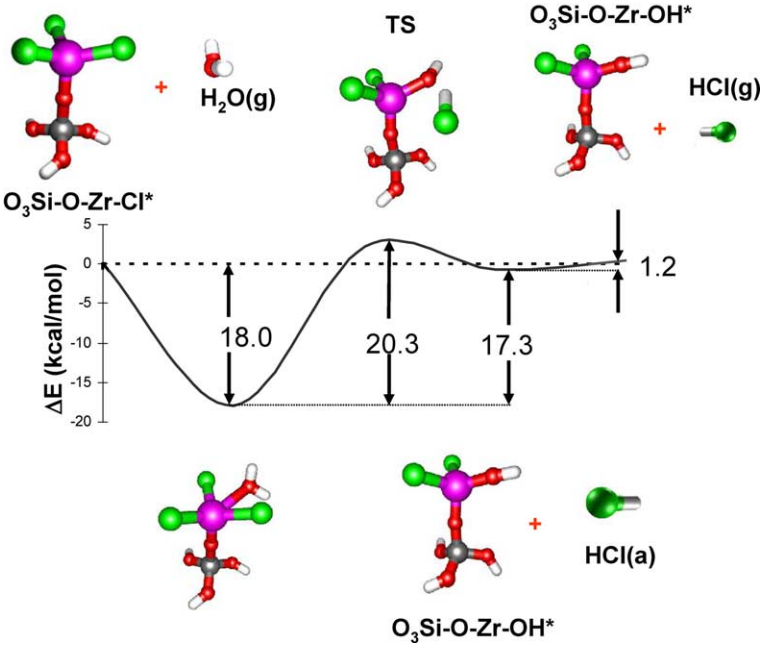

Fig. 3. Reaction path and predicted energetics for the reaction of H_2O on SiO_2–O–$ZrCl_3^*$ sites. The purple, gray, red, green, and white atoms denote the zirconium, silicon, oxygen, chlorine and hydrogen atoms, respectively. (For interpretation of the references in colour in this figure legend, the reader is referred to the web version of this article.)

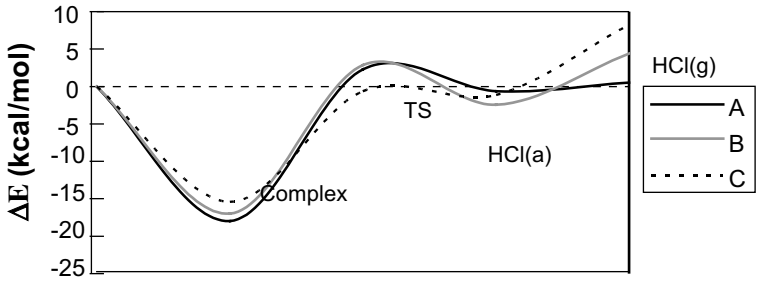

Fig. 4. PESs of H_2O reaction with all three Cl atoms on Zr, calculated using the $Si(OH)_3SiOZrCl_3$ cluster for (A) removal of the first Cl atom, (B) removal of the second Cl atom, and (C) removal of the third Cl atom.

atoms by OH groups and evolution of HCl. The second and third Cl removal reactions are presented respectively as follows:

$$Si(OH)_3\text{–}O\text{–}Zr(OH)Cl_2^* + H_2O \rightarrow Si(OH)_3\text{–}O\text{–}Zr(OH)_2Cl^* + HCl$$

$$Si(OH)_3\text{–}O\text{–}Zr(OH)_2Cl^* + H_2O \rightarrow Si(OH)_3\text{–}O\text{–}Zr(OH)_3^* + HCl$$

The PESs for removal of all the three Cl atoms are shown in Fig. 4. Geometric parameters of interest illustrated in Fig. 5, such as the Zr–Cl bond length of the water complexes, the distance between HCl(a) and the O of the Zr–OH^* sites, and the minimum distance between the HCl(a) and the H atoms used to terminate the Si–O bonds are summarized in Table 1. Formation of the absorbed complex is exothermic by 18.0 kcal/mol for SiO_2–O–$ZrCl_3$–H_2O(a), 17.0 kcal/mol for SiO_2–

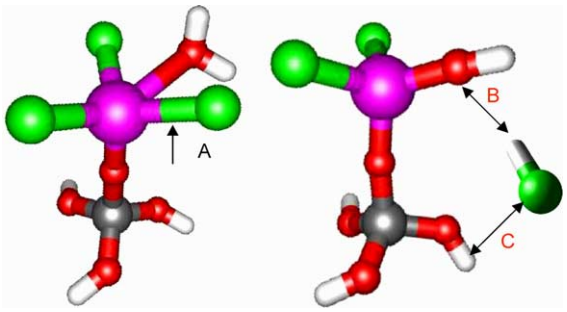

Fig. 5. Illustration of parameters shown in Table 1: (A) Zr–Cl bond of the adsorbed water complex, (B) the distance between HCl(a) and the O atom of the Zr–OH* site, and (C) the minimum distance between HCl(a) and H atoms used to terminate the Si–O bond.

O–Zr(OH)Cl_2–H_2O(a) and 15.4 kcal/mol for SiO_2–O–Zr$(OH)_2$Cl–H_2O(a). Relative to the water complex, the activation barriers for HCl formation are 20.3, 19.8, and 14.8 kcal/mol for the first, second, and third Cl removal, respectively.

The lower activation barriers for the removal of the second and third Cl atoms are the result of successive weakening of the Zr–Cl bond by the increasing number of OH groups bonded to the Zr atom. As shown in Table 1, the Zr–Cl bond length of the water complex increases from 2.48 Å for the first Cl to 2.52 and 2.53 Å for the second and third Cl atoms, respectively. One possible explanation of this effect is that donation of the O lone pair into an empty d-orbital of the Zr atom in addition to the covalent bonds between the Zr atom and the O atoms weakens the Zr–Cl bonds. This electron donation effect can also explain the weakening of the H_2O absorbed complex with the increasing number of OH groups bonded to the Zr atom, manifested by the change in the water complex formation energy, as mentioned above.

The desorption energy of physisorbed HCl is 1.2 kcal/mol for removal of the first Cl, 6.8 kcal/mol for removal of the second Cl and 9.4 kcal/mol for removal of the third Cl. The progressive increase in the HCl desorption energy for removal of the second and third Cl atoms can be partially explained by the increased stability of the physisorbed HCl that results because the OH group that replaces the Cl atom occupies less space than the Cl atom and thus results in less steric interactions. This in turn allows closer bonding of the HCl(a) to the surface Zr–OH* sites, as evident from the decrease in the distance between HCl(a) and the O atom of the Zr–OH* site that replaces the Zr–Cl* site. Another cause for the increase in desorption energy is the error introduced by using a small cluster for the calculation. As shown in Table 1, the distance between the Cl atom of HCl(a) and the nearest H atom used to terminate the Si–O bonds changed from 2.46 Å for removal of the first Cl atom, to 2.44 Å for removal of the second Cl atom, to 2.42 Å for removal of the third Cl atom. This error can be corrected by using a larger cluster for the calculation, as shown below.

Table 1
Comparison of Zr–Cl bond length of the water complex, distance between the HCl(a) and O of the Zr–OH* sites and the minimum distance between HCl(a) and H atoms used to terminate the Si–O bond for removal of the three Cl atoms bonded to Zr–Cl* surface sites

Complex	Zr–Cl bond length (Å)	Distance between HCl (a) and O of Zr–OH* site (Å)	Minimum distance between HCl(a) and H atoms used to terminate the Si–O bond (Å)
$Si(OH)_3OZrCl_3$ cluster			
$Si(OH)_3OZrCl_3$–H_2O	2.48	1.78	2.46
$Si(OH)_3OZr(OH)Cl_2H_2O$	2.52	1.69	2.44
$Si(OH)_3OZr(OH)_2Cl$–H_2O	2.53	1.58	2.42
$(SiH_3O)_3SiOZrCl_3$ cluster			
$(SiH_3O)_3SiOZrCl_3$–H_2O	2.45	1.84	3.56
$(SiH_3O)_3SiOZr(OH)Cl_2$–H_2O	2.48	1.81	7.24
$(SiH_3O)_3SiOZr(OH)_2Cl$–H_2O	2.50	1.68	3.76

3.3. The effect of cluster truncation

To investigate the cluster size effect on the reaction energetics, calculations were performed to compare the stationary points on the PESs for the reaction of gaseous $ZrCl_4$ on SiO_2–OH^* surface sites using the $Si(OH)_3$–OH, $SiH_3OSi(OH)_2$–OH and $(SiH_3O)_3Si$–OH clusters. Results are shown in Fig. 6. The reaction mechanism is found to be the same for all three clusters. The energy for the formation of the adsorbed complex is −16.9 kcal/mol with the $Si(OH)_3$–OH cluster, −17.8 kcal/mol with the $SiH_3OSi(OH)_2$–OH cluster and −17.8 kcal/mol with the $(SiH_3O)_3Si$–OH cluster. The energy of the overall reaction calculated using the three clusters also varied by a maximum of 0.9 kcal/mol. The largest difference in energy is observed between values calculated using the $Si(OH)_3$–OH and the $SiH_3OSi(OH)_2$–OH clusters. Energies calculated using an even larger cluster, $(SiH_3O)_3Si$–OH, only showed a 0.8 kcal/mol deviation from the results calculated with $Si(OH)_3$–OH, which is the smallest cluster. Cluster size had no effect on the calculated activation barrier for HCl formation. Consequently, the reaction of $ZrCl_4$ on the SiO_2 surface does not exhibit significant non-local effects and the smaller $Si(OH)_3$–OH cluster is a good model of the surface active sites since it is sufficient to describe the surface reaction at single hydroxyl sites.

We also calculated the reaction energetics for the reaction of H_2O on the SiO_2–O–$ZrCl_3^*$ surface site using three different clusters. Since the active bond is even more removed from the surface than in the case of the SiO_2–OH^* active site, even less of a cluster size effect is expected. Results are given in Fig. 7. $Si(OH)_3OZrCl_3$, $SiH_3OSi(OH)_2OZrCl_3$ and $(SiH_3O)_3SiOZrCl_3$ clusters, representing products of the first half-reaction using the $Si(OH)_3$–OH, $SiH_3OSi(OH)_2$–OH and $(SiH_3O)_3Si$–OH clusters, were used in the calculation. The results showed negligible differences. The insensitivity of the reaction energetics to the size of the SiO_2 cluster demonstrates that the reaction of water on the SiO_2–O–$ZrCl_3^*$ site does not exhibit significant non-local effects, as one would expect.

Fig. 8 shows the PES for removal of all the three Cl atoms bonded to Zr calculated using the $(SiH_3O)_3SiOZrCl_3$ cluster. The patterns are similar to that calculated using the smaller $Si(OH)_3OZrCl_3$ cluster shown in Fig. 4. Table 2 compares the energetics calculated using the two different clusters. The smaller cluster gives rise to a varying activation barrier for the formation of

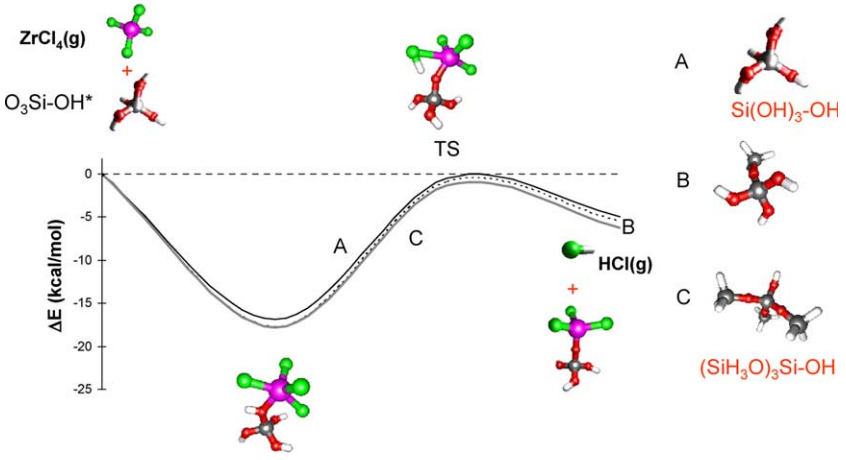

Fig. 6. Comparison of reaction paths and predicted energetics for the reaction of gaseous $ZrCl_4$ on the SiO_2–OH^* sites calculated using (A) $Si(OH)_3$–OH cluster, (B) $SiH_3OSi(OH)_2$–OH cluster, and (C) $(SiH_3O)_3Si$–OH cluster, showing cluster size effect on the results. The purple, gray, red, green, and white atoms denote the zirconium, silicon, oxygen, chlorine and hydrogen atoms, respectively. (For interpretation of the references in colour in this figure legend, the reader is referred to the web version of this article.)

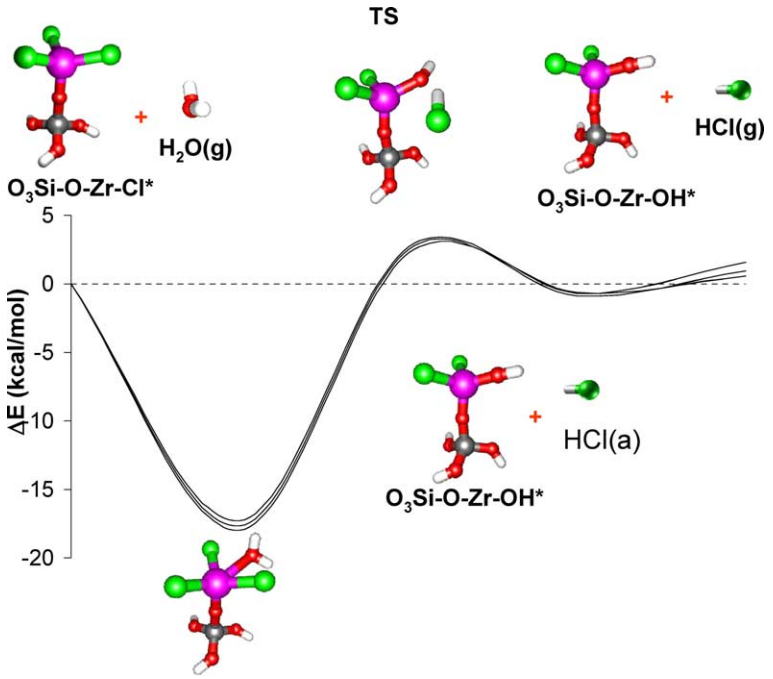

Fig. 7. Comparison of reaction path and predicted energetics for the reaction of H_2O on the SiO_2–O–Zr–Cl_3^* sites calculated using (a) $Si(OH)_3OZrCl_3$ cluster, (b) $SiH_3OSi(OH)_2OZrCl_3$ cluster, and (c) $(SiH_3O)_3SiOZrCl_3$ cluster, showing the cluster effect on the results. The purple, gray, red, green, and white atoms denote the zirconium, silicon, oxygen, chlorine and hydrogen atoms, respectively. (For interpretation of the references in colour in this figure legend, the reader is referred to the web version of this article.)

physisorbed HCl and a higher HCl desorption energy. As mentioned in Section 2, the error from using the smaller cluster is due to interference of H atoms used to terminate the subsurface Si–O bonds. The close proximity between these H atoms and the physisorbed HCl alters the transition state barrier and increases the desorption energy. However, the maximum difference calculated is only 2.7 kcal/mol, which is not large enough to alter the nature of the reaction mechanism.

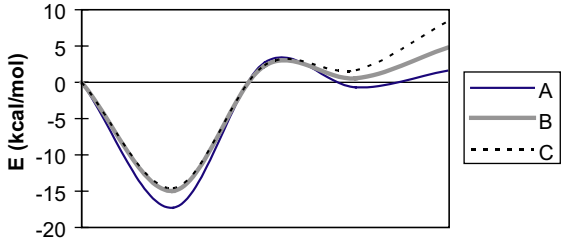

Fig. 8. PESs calculated using the $(SiH_3O)_3SiOZrCl_3$ cluster for reaction of (A) removal of the first Cl atom, (B) removal of the second Cl atom, and (C) removal of the third Cl atom.

With the $(SiH_3O)_3SiOZrCl_3$ cluster, the interaction between the H atoms used to terminate the subsurface Si–O bonds and the gaseous precursors is negligible. As shown in Table 1, the distance between the Cl atom of the physisorbed HCl and nearest H atom used to terminate the Si is increased to 3.56 Å.

As we have shown in Section 2, when a small cluster is used for the calculation, the H atoms used to terminate the subsurface Si–O bonds may interfere with the calculation and induce a small error in the calculated energetics. To more realistically simulate the reaction on a rigid surface, constraints on the subsurface can be added during the transition state searches for both half-reactions. Unless stated otherwise, the $Si(OH)_3$ group, which represents the surface and is not directly involved in the reaction was fixed during the first step of transition state calculation. The constraints

Table 2
Comparison of energetics (in kcal/mol) calculated using different size clusters for the Si–O–$Zr(OH)_{3-x}$–Cl_x^* + H_2O reactions

	Zr–Cl^*–H_2O complex	TS	Zr–OH^*–HCl complex	HCl desorption
SiO_2–O–$ZrCl_3$ + $H_2O \rightarrow SiO_2$–O–$Zr(OH)Cl_2$ + HCl				
$Si(OH)_3OZrCl_3$ cluster	−17.9	20.3	17.3	1.2
$(SiH_3O)_3SiOZrCl_3$ cluster	−17.3	20.0	16.6	2.3
SiO_2–O–$Zr(OH)Cl_2$ + $H_2O \rightarrow SiO_2$–O–$Zr(OH)_2Cl$ + HCl				
$Si(OH)_3OZr(OH)Cl_2$ cluster	−17.0	19.8	14.6	6.8
$(SiH_3O)_3SiOZr(OH)Cl_2$ cluster	−15.0	17.2	15.5	4.2
SiO_2–O–$Zr(OH)_2Cl$ + $H_2O \rightarrow SiO_2$–O–$Zr(OH)_3$ + HCl				
$Si(OH)_3OZr(OH)_2Cl$ cluster	−15.4	14.8	14.3	9.4
$(SiH_3O)_3SiOZr(OH)_2Cl$ cluster	−14.6	16.9	16.2	6.7

Energies of the Zr–Cl^*–H_2O are relative to the entrance channel. Energies of TS, Zr–OH^*–HCl complex are relative to the Zr–Cl^*–H_2O complex. Energies of HCl desorption are relative to the Zr–OH^*–HCl complex.

limited movement of the H atoms used to terminate the Si–O bonds and guided the transition state calculation to the right saddle points. This resulted in a structure with multiple negative frequencies due to rotation of the constrained O–H bonds. Once the transition state was found, the constraints on the $Si(OH)_3$ group were removed. Repeating the transition state calculation with the cluster fully relaxed allowed relaxation of the H atoms and eliminated the negative frequencies mentioned above associated with the constrained H atoms. The result was a structure with only one negative frequency.

3.4. Comparison of ZrO_2 growth on SiO_2, ZrO_2 and the OH terminated Si surface

Figs. 9 and 10 show the comparison of PESs for the deposition of ZrO_2 on the OH terminated Si surface, ZrO_2 and SiO_2. We use Zr–OH^* and Si–OH^* to denote hydroxylated ZrO_2 and Si surfaces, respectively. Similarly, Zr–O–$ZrCl^*$ and Si–O–$ZrCl^*$ denote the products of $ZrCl_4$ adsorption on the respective Zr–OH^* and Si–OH^* surfaces. The PESs representing surface reactions of $ZrCl_4$ and H_2O on SiO_2 and ZrO_2 surface sites show little difference. Clearly, very little qualitative energetic difference exists for the initiation of the first monolayer of ZrO_2 on SiO_2 and subsequent thickening of ZrO_2 because the reactions do not show significant non-local effects, as previously discussed.

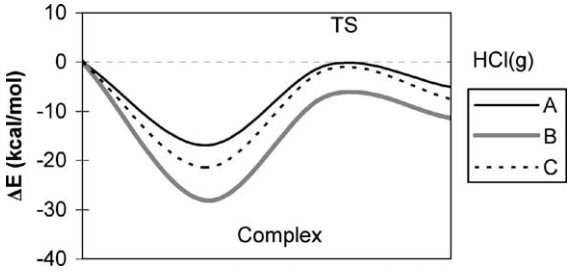

Fig. 9. Comparison of reaction energetics for $ZrCl_4$ reaction on the (A) SiO_2–OH^* surface site, (B) Zr–OH^* surface site, and (C) Si–OH^* surface site.

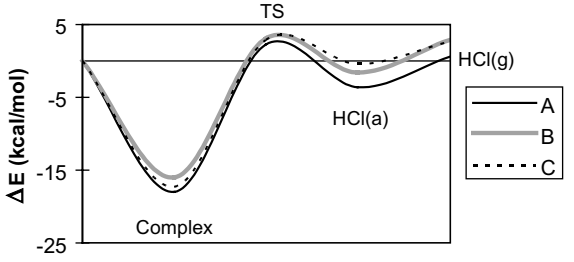

Fig. 10. Comparison of reaction energetics for H_2O reaction on the (A) SiO_2–O–$ZrCl_3^*$ surface site, (B) Zr–O–$ZrCl_3^*$ surface site, and (C) Si–O–$ZrCl_3^*$ surface site.

However, even though the shape of the PESs are similar for the different surfaces, differences in the relative energies are present. Compared with the reaction of $ZrCl_4$ on hydroxylated SiO_2, reaction of $ZrCl_4$ on hydroxylated Si resulted in a 4.5 kcal/mol lower formation energy for the absorbed

complex, a 3.6 kcal/mol higher energy for the transition state activation barrier and a 2.1 kcal/mol higher energy for the HCl desoprtion. For the second half-reaction, the energy for the intermediate complex formation is 0.7 kcal/mol higher, the activation barrier is 0.1 kcal/mol lower, and the HCl desorption energy is 1.4 kcal/mol higher for the reaction on the Si surface. The energetics of ZrO_2 deposition on hydroxylated SiO_2 do not deviate qualitatively from ZrO_2 deposition on the –OH terminated Si surface; however, depending upon the reactor temperature, differences on the order of 5 kcal/mol could be sufficient to change the growth rate.

One distinctive characteristic of both half-reactions involves the formation of a stable intermediate complex, regardless of the initial surface condition. Widjaja and Musgrave [11,12] have shown that the complexes are formed through the interaction between an oxygen lone-pair and an empty d-orbital of Zr. For the first half-cycle, the lone-pair electrons come from the oxygen of the hydroxylated Si, ZrO_2 and SiO_2 surfaces (Si–OH^*, Zr–OH^* and SiO_2–OH^* sites), respectively, and the Zr atom comes from the $ZrCl_4$ precursor molecule. For the second half-cycle, the lone-pair electrons come from the oxygen of H_2O and the Zr atom comes from the Si–O–$ZrCl^*$, the Zr–O–$ZrCl^*$ or the SiO_2–O–$ZrCl^*$ surface sites. The electron donation from an oxygen lone-pair to the empty d-orbital of the Zr atom is relatively exothermic, resulting in adsorption energies of −21.4 kcal/mol for $ZrCl_4$ adsorption on Si–OH^*, −28.1 kcal/mol for $ZrCl_4$ adsorption on Zr–OH^*, −16.9 kcal/mol for $ZrCl_4$ adsorption on SiO_2–OH^*, −17.3 kcal/mol for H_2O adsorption on Si–O–$ZrCl_3^*$, −16.0 kcal/mol for H_2O adsorption on Zr–O–$ZrCl_3^*$, and −18.0 kcal/mol for H_2O adsorption on SiO_2–O–$ZrCl_3^*$ surface sites, respectively.

As reported previously [12], the free energies of the complex shift up with respect to the initial precursor state and the final state with increasing temperature. This results in reduced stability of the complex intermediates. Around 600 K, the associated product free energies become lower than the adsorbed intermediate free energies. This shows that raising the temperature shifts the equilibrium concentration from the complex towards the products. However, at high temperatures, the activation free energy for the desorption of the adsorbed precursor molecule becomes smaller than the activation free energy for the formation of HCl. As a result, the rate of desorption may increase faster than the rate of HCl elimination as the temperature is increased. High reactant pressures can be used to increase the time-averaged concentration of adsorbed precursors to shift equilibrium towards the products. However, under actual growth conditions, it is likely that gas-surface equilibrium is not attained, and that with a high flow rate of gases over the substrate, reaction by-products such as HCl are removed from the chamber without substantial readsorbtion helping drive the reaction forward while moving the system away from equilibrium. Although equilibrium is most likely not achieved under actual flow conditions, the shifts in equilibrium caused by changes in temperature, pressures, and flow rates can be determined based on the potential energy surfaces we have reported herein.

3.5. Reaction of $ZrCl_4$ with multiple SiO_2–OH^* surface sites

The PES of the reaction of $ZrCl_4$ with multiple surface sites is more complex because of the branching of reaction pathways. Fig. 11 shows the reactions of $ZrCl_4$ with two surface Si–OH^* groups. Initally, the $ZrCl_4$ molecule has two oxygen lone-pair interactions with the two surface hydroxyl groups (black line). The intermediate is 30.8 kcal/mol below the entrance channel, which is nearly double the 16.9 kcal/mol seen with a single surface hydroxyl site. The activation barrier to the formation of HCl is 25.8 kcal/mol relative to the energy of the adsorbed intermediate. The HCl product can be weakly physisorbed with an energy that is 13.3 kcal/mol above the adsorbed complex, and the desorption energy for HCl is endothermic by 3.5 kcal/mol.

After the elimination of the first HCl, the reaction network can branch. One alternative would be for the zirconium atom to remain 5-fold coordinated (three bonds to Cl atoms and two dative bonds from the surface hydroxyl groups)

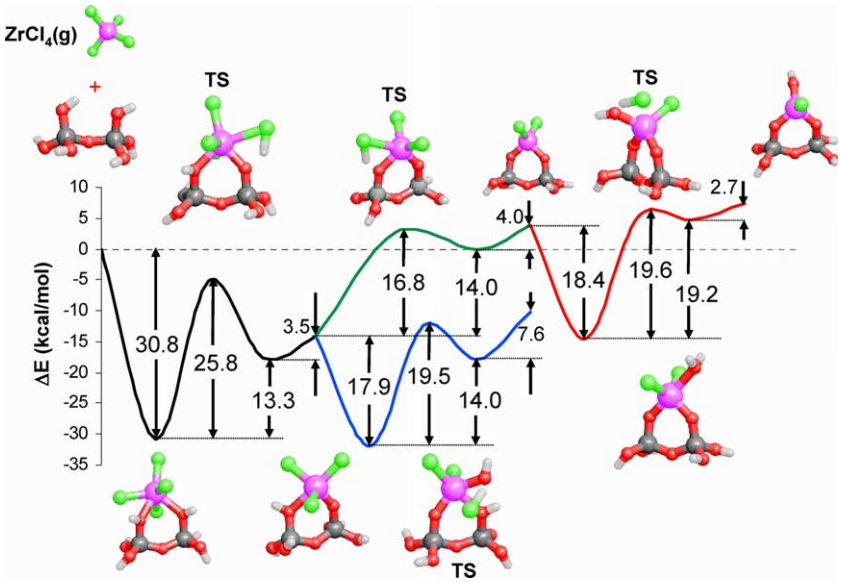

Fig. 11. Reaction path and predicted energetics for the reaction of $ZrCl_4$ on multiple surface hydroxyl sites using a $Si(OH)_2$–OH^*–O–$Si(OH)_2$–OH^* cluster. The green pathway represents the elimination of a second HCl from the adsorbed $ZrCl_4$. The blue and red pathways represent the second ALD half-reaction with water. The purple, gray, red, green, and white atoms denote the zirconium, silicon, oxygen, chlorine and hydrogen atoms, respectively. (For interpretation of the references in colour in this figure legend, the reader is referred to the web version of this article.)

for the second ALD half-reaction with water (Fig. 11, blue line). As in the previous calculations with only one surface hydroxyl group, water can adsorb via a lone-pair donation to the zirconium atom. Formation of this stable complex is exothermic by 17.9 kcal/mol. The transition state to the formation of HCl has an energy 19.5 kcal/mol relative to the adsorbed state, and the reaction is endothermic by 14.0 kcal/mol relative to the complex. The HCl desorption energy is 7.6 kcal/mol uphill relative to the physisorbed state. Compared to the cluster model with only one surface hydroxyl group, the adsorbed complex and transition state energies are nearly identical. The physorbed HCl, however, is approximately 3 kcal/mol more stable due to an additional interaction with the second surface hydroxyl group. This leads to a slightly more stable HCl physisorbed state and a higher HCl desorption energy.

An alternative to the 5-fold coordinated water half-reaction pathway would be for the surface zirconium atom to eliminate a second HCl through reaction with a surface hydroxyl group (Fig. 11, green line). From the product of the first HCl elimination, there is a 16.8 kcal/mol barrier to the formation of the second HCl product. The HCl can remain physisorbed in a state that is 14.0 kcal/mol above the product of the first HCl elimination; the desorption of the second HCl is endothermic by 4.0 kcal/mol. Again, the energies of the critical points of this pathway are nearly identical to those described previously where the model only allowed for a single surface hydroxyl group interaction.

From the product of the second HCl elimination, water can react with the $ZrCl_2$ surface species by the second half-reaction of the ALD process (Fig. 11, red line). The adsorption energy of water on this surface is 18.4 kcal/mol. The energy of the transition state for the formation of HCl is 19.6 kcal/mol above the adsorbed complex. The physisorbed HCl state is 19.2 kcal/mol above the lone-pair donation complex. The desorption energy of HCl is 2.7 kcal/mol.

For the most part, the kinetics, which are related to the energy differences between the transition states and the adsorbed complexes, of the

ALD growth reactions are not affected significantly by the interaction of the incoming $ZrCl_4$ with multiple surface hydroxyl groups. The major differences are that for the first half-reaction where the first HCl is eliminated the second Zr–O dative bond shifts the exchange reaction PES down approximately 14 kcal/mol, which decreases the probability of precursor desorption, and increases the barrier for the exchange reaction by 9.4 kcal/mol relative to the adsorbed complex. However, the stabilities of the intermediates and transition states for two half-reactions is increased when the coordination number of the zirconium atom of the reacting precursor is increased by additional interactions with surface sites, ligands, and other adsorbing gas phase molecules. For example, for the second half-reaction where –Cl is exchanged with a –OH, the additional –Cl ligand shifts the ligand-exchange reaction PES down approximately 18 kcal/mol while the barrier relative to the complex is nearly constant at 19.5 kcal/mol.

3.6. Reaction of $ZrCl_4$ with SiO_2–OH^* surface sites on a 1-dimer cluster

The PES of the reaction of $ZrCl_4$ as shown above is not sensitive to the cluster model. However, our results differ from those published previously [10]. In that work, a similar pathway is explored; however, the relative energies are different. To reconcile the differences, calculations using our methodology were performed on the silicon 1-dimer clusters where the top layer has been oxidized.

For the initial adsorbed complex, we find the adsorption energy to be 15.0 kcal/mol. This is weaker than we found previously using a pure hydroxylated SiO_2 surface (16.9–17.8 kcal/mol). The difference likely arises from the geometric constraints used in the 1-dimer model compared to the unconstrained SiO–OH^* clusters. Jeloacia found the adsorption energy to be only 10.0 kcal/mol. This difference of 5 kcal/mol is likely due to differences in cluster geometry and basis set.

For the transition state energy, we find the barrier to be 15.1 kcal/mol above the adsorbed state. The transition state is less than 0.5 kcal/mol away from the entrance channel as observed for the unstrained clusters. Our barrier is lower than the 20.1 kcal/mol barrier obtained by Jeloacia. If the choices of cluster geometry and basis set led to systematic differences in relative energies, one would expect a similar barrier; however, the differences appear to be increasing. Jeloacia used an iterative transition state search approach called bond constraint relaxation (BCR) where the reaction coordinate and non-reaction coordinate degrees of freedom are alternately optimized. This limits the ability to fully explore the potential energy surface of the system to locate the transition state. The transition state search algorithm in Gaussian simultaneously minimizes the energy of the system while searching for a mathematical first-order saddle point with the negative frequency corresponding to the reaction coordinate. The BCR technique obtains a reaction barrier that is an upper bound to the true value while the technique employed in Gaussian leads to a barrier that is most likely closer to the true value.

4. Conclusions

The atomistic mechanism of growth of first monolayer of ZrO_2 on hydroxylated SiO_2 by ALD using $ZrCl_4$ and H_2O precursors has been investigated. The reaction pathways consist of two half-cycle reactions: (1) $ZrCl_4$ reacts with the SiO_2–OH^* surface sites, which results in SiO_2–O–$ZrCl^*$ sites, and (2) H_2O reactions with SiO_2–O–$ZrCl^*$ surface sites, resulting in SiO_2–O–Zr–OH^* sites.

The reaction energetics of ZrO_2 deposition on hydroxylated SiO_2 are qualitatively similar to the energetics of ZrO_2 deposition on the growing ZrO_2 film and the energetics of ZrO_2 deposition on hydroxylated Si. The intermediate complex formed by absorption of the gaseous precursor, $ZrCl_4$ and H_2O, are more stable than the final state. This will result in trapping both half-reactions in the intermediate state. Increasing the reaction temperature and pressure of the gaseous precursors shifts the overall equilibrium from the stable absorbed precursor state to the final state. However, as in the case of the homogeneous ALD of ZrO2, increasing the temperature leads to desorption of precursor and submonolayer growth. The reaction pathways for $ZrCl_4$ reaction with multiple surface hydroxyl

sites exhibit similar reaction mechanisms as those on a single site; however, the additional dative bond to the Zr atom stabilizes the adsorbed complex and products while increasing the barrier for the first exchange reaction.

Acknowledgements

The authors thank Professor Jeung Ku Kang, Dr. Collin Mui, and Dr. Juan Senosiain for their help. Support of this work by the Ford Motor Company, National Science Foundation Graduate Research Fellowship, the Stanford Center for Integrated Systems, Semiconductor Research Corporation, MSD Marco Center, the Office of Naval Research, and the Powell Foundation are gratefully acknowledged. This research was also supported through computing resources provided by the National Center for Supercomputing Applications (NCSA).

References

[1] P.A. Packan, Science 285 (1999) 2079.
[2] M. Copel, M. Gribelyuk, E. Gusev, Appl. Phys. Lett. 76 (2000) 436.
[3] M. Ritala, N. Leskela, in: H.S. Nalwa (Ed.), Handbook of Thin Film Materials, vol. 1, Academic Press, New York, 2001 (Chapter 2).
[4] H. Zhang, R. Solanki, B. Roberds, G. Bai, I. Banerjee, J. Appl. Phys. 87 (2000) 1921.
[5] C.M. Perkins, B.B. Triplett, P.C. McIntyre, K.C. Saraswat, S. Haukka, M. Tuominen, Appl. Phys. Lett. 78 (2001) 2357.
[6] J. Aarik, A. Aidla, H. Mandar, T. Uustare, V. Sammelselg, Thin Solid Films 408 (2002) 97.
[7] K. Kukli, M. Ritala, J. Aarik, T. Uustare, M. Leskela, J. Appl. Phys. 92 (2002) 1833.
[8] A. Esteve, M. Rouhani, L. Jeloaica, D. Esteve, Comput. Mater. Sci. 27 (2003) 75.
[9] A. Rahtu, M. Ritala, J. Mater. Chem. 12 (2002) 1484.
[10] L. Jeloaica, A. Esteve, M. Rouhani, D. Esteve, Appl. Phys. Lett. 83 (2003) 542.
[11] Y. Widjaja, C.B. Musgrave, J. Phys. Chem. B 107 (2003) 9319.
[12] Y. Widjaja, C.B. Musgrave, Appl. Phys. Lett. 81 (2002) 304.
[13] J.H. Han, C.B. Musgrave, in preparation.
[14] L.A. Eriksson, L.G.M. Pettersson, P.E.M. Siegbahn, U. Wahlgren, J. Chem. Phys. 102 (1995) 872.
[15] P.J. Hay, W.R. Wadt, J. Chem. Phys. 82 (1985) 270.
[16] P.J. Hay, W.R. Wadt, J. Chem. Phys. 82 (1985) 299.
[17] W.R. Wadt, P.J. Hay, J. Chem. Phys. 82 (1985) 284.
[18] T.H. Dunning Jr., P.J. Hay, in: H.F. HSchaefer III (Ed.), Modern Theoretical Chemistry, Plenum, New York, 1976.
[19] M.J. Frisch et al., Gaussian 98, Revision A.11.2, Pittsburgh, PA, 2001.